INL/CON-15-37501
PREPRINT

Wall Area of Influence and Growing Wall Heat Transfer due to Sliding Bubbles in Subcooled Boiling Flow

11th International Topical Meeting on Nuclear Thermal-Hydraulics, Operation and Safety (NUTHOS-11)

Junsoo Yoo, Carlos E. Estrada-Perez,
Yassin A. Hassan

April 2016

The INL is a
U.S. Department of Energy
National Laboratory
operated by
Battelle Energy Alliance

Wall Area of Influence and Growing Wall Heat Transfer due to Sliding Bubbles in Subcooled Boiling Flow

Junsoo Yoo*
Idaho National Laboratory
2525 North Fremont Ave. P.O.Box 3860, Idaho Falls, Idaho, USA (Zip: 83415)
junsoo.yoo@inl.gov

Carlos E. Estrada-Perez, Yassin A. Hassan
Texas A&M University
Department of Nuclear Engineering, 3133 TAMU, College Station, Texas, USA (Zip: 77840)

ABSTRACT

A variety of dynamical features of sliding bubbles and their impact on wall heat transfer were observed at subcooled flow boiling conditions in a vertical square test channel. Among the wide range of parameters observed, we particularly focus in this paper on (i) the sliding bubbles' effect on wall heat transfer (supplementary discussion to the authors' previous work in *Yoo et al. (2016)*) and (ii) the wall area influenced by sliding bubbles in subcooled boiling flow. This study first reveals that the degree of wall heat transfer improvement caused by sliding bubbles depends less on the wall superheat condition as the mass flux increased. Also, the sliding bubble trajectory is found to be critical to describe the wall heat transfer associated with sliding bubbles after departure from a single nucleation site. In particular, the wall area influenced by sliding bubbles depends strongly on both sliding bubble trajectory and sliding bubble size; the sliding bubble trajectory is also observed to be closely related to the sliding bubble size. Importantly, these results indicate the limitation of current approach in CFD analyses for the wall area of bubble influence. In addition, the analyses on the temporal fraction of bubbles' residence (F_R) on the heated wall show that the sliding bubbles typically travel through narrow path with high frequency near the nucleation site while the opposite was observed downstream. That is, both F_R and sliding bubble trajectory depends substantially on the distance from nucleation site, which is expected to be similar for the quenching heat transfer mode induced by sliding bubbles.

KEYWORDS

Subcooled boiling flow, bubble sliding, boiling heat transfer, single nucleation site

1. INTRODUCTION

The significance of sliding bubbles' effect on wall heat transfer has been proved through experiments by previous researchers [1-3]. Due to the importance of sliding bubbles in surface cooling aspect, efforts have been made to address the effect through modelling [4, 5]. However, the fundamental mechanism of the wall heat transfer associated with sliding vapor bubbles is yet to be well understood and thus it is still among the topics of great interest within boiling heat transfer community.

This paper mainly discusses the wall heat transfer induced by sliding bubbles based on the observation from a subcooled flow boiling experiment. The experiment was performed by creating only a single active nucleation site within test channel to clearly observe the sliding bubbles' characteristic and thermal effect by high-speed cameras as well as infrared camera. It is noted that the various characteristics of sliding bubbles' behavior and associated wall heat transfer observed from this experiment are largely discussed in Yoo et al. [6, 7]. In this paper, we made supplementary discussion

based on the recent findings achieved while analyzing the experimental data in different aspect. In addition, the wall area (or bubble influence factor) influenced by sliding bubbles, which is considered an important factor from the viewpoint of wall heat flux partitioning model [5, 8], is another major part of discussion. We concluded from this study that the bubbles' sliding trajectory after departure from a nucleation site needs to be carefully addressed and characterized to correctly determine the wall area influenced by sliding bubbles.

Considering that there exists little evidence or fundamental study on the sliding bubbles' trajectory and the thermal influential area, the experimental findings described in this paper will help significantly improve our insight into the sliding bubbles' effect in subcooled boiling flow.

2. TEST LOOP AND BOILING MEASUREMENT STRATEGY

2.1. Test Loop

Detailed information on the test loop for the present subcooled flow boiling experiment is described in Ref. [6]. In this section, the main feature of the experimental setup is briefly described. The subcooled flow boiling experiment was performed in a vertical, square, upward flow channel. The refrigerant Novec-7000 (3M Inc.) was used as a working fluid. The four sides of test section walls were made of transparent materials (transparent to visible light) with the heater wall on one side. On the heater wall side, ITO was deposited on top of glass substrate so that a heat can be provided to the test channel through Joule heating. ITO was adopted as a heating element because of its special optical property (*i.e.*, transparent to visible light and opaque to infrared radiation), allowing us to measure the heater surface (hereafter, wall) temperature using infrared (IR) camera without damaging the quality of high-speed bubble imaging. The test section flow area was 10×10 mm^2 while the heated surface area on the heater wall side was 7.5×224 mm^2. The experiment was performed with the range of mass flux (G) 140-700 kg/m^2s, inlet subcooling ($\Delta T_{sub,in}$) 4.5-13.5 ℃, and wall heat flux (q_w) 8.1-35.1 kW/m^2.

It is noted that during this study only a single artificial nucleation site was activated at the axial location $L/L_0 \approx 0.41$ (L_0 is the total heated length and L is the axial location within L_0). This was to enhance the observation of bubbles and associated wall heat transfer through the optical measurement techniques employed in this work by controlling the complexity of boiling phenomena. More specifics on the strategy for the present boiling experiment are described in the following section.

2.2. Experimental Strategy

The high-speed bubble imaging and infrared (IR) thermometry has been simultaneously applied to observe the bubble and wall heat transfer parameters at subcooled flow boiling conditions. The experimental method to achieve both accurate wall temperature measurement (using IR thermometry) and enhanced flow visualization have been established from our previous work [9], including extensive validations for IR measurement accuracy. Also, several measurement issues of high-speed bubble imaging is discussed in [10] in which an automatic image analysis algorithm is also developed. Then, by incorporating all these efforts we could achieve truly high-fidelity data from the present flow boiling experiment. In Figure 1, the established techniques which serve to enhance the present data quality is summarized.

In addition, we took a unique strategy during the present subcooled flow boiling experiment to overcome the general difficulties of optical measurement under boiling condition, as presented in Figure 2. Considering that the high phenomenological complexity and the optical distortion caused by boiling usually prevent us from observing the underlying physics, we controlled the number of nucleation site as single (*i.e.*, bottom-up approach). Also, the bubbles' behavior was captured with multiple scales (*i.e.*, high- and low-resolutions) to investigate the aspects of bubble characteristics (multi-scale observation). Moreover, a variety of parameters were observed together, allowing us to gain better insight into the relation among the measured parameters (multi-variable measurement). The

effects of test boundary conditions (*e.g.*, mass flux, subcooling degree, wall heat flux) on bubbles' characteristic and associated wall heat transfer were systematically observed. Lastly, efforts were made to analyze the numerous images to characterize the 'typical' bubble behavior and wall heat transfer at a given condition with high statistical significance. More details on the present experiment and the data quality achieved are presented in Yoo et al. [6].

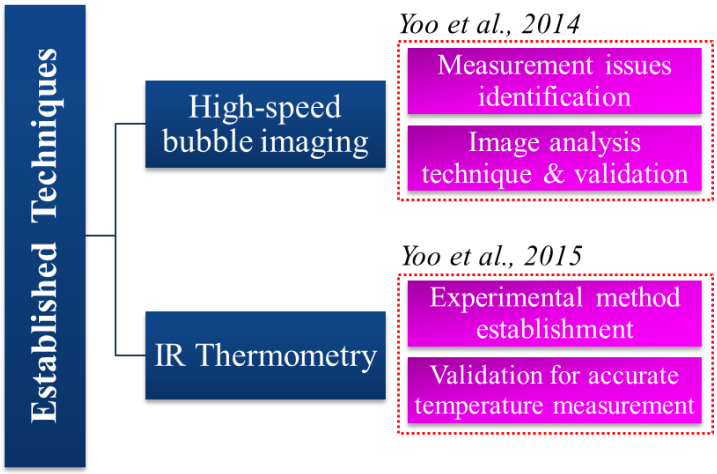

Figure 1. Established experimental techniques for achieving high-fidelity optical measurement

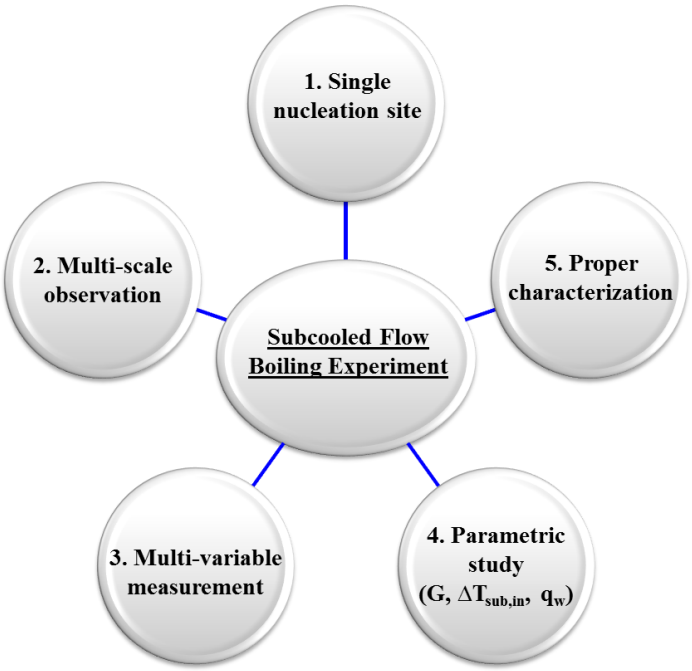

Figure 2. Strategy for enhancing the observation of subcooled flow boiling characteristics [6]

3. AVAILABLE RESEARCH SCOPE AND CURRENT INTEREST

The experimental strategy described in section 2 allowed in-depth observation of extensive range of parameters under subcooled flow boiling conditions. Since the bubbles observed during this work mostly slid along the heated wall after departure from the nucleation site, the research scope mainly covers the sliding bubbles' characteristics and their impact on wall heat transfer. The specific interests include sliding bubbles' growth behavior, sliding bubble velocity, sliding bubbles' coalescence, wall heat transfer induced by sliding bubbles, and size distribution of sliding bubbles, etc., as illustrated in Figure 3. The detailed discussion based on the observation of those parameters are given in Ref. [7].

In this paper, the experimental findings from the present subcooled flow boiling experiment is further discussed by focusing more on sliding bubbles' effect on wall heat transfer. The discussion includes (i) supplementary analyses to the previous work described in Ref. [7] regarding wall heat transfer enhancement induced by sliding bubbles (section 4.1), (ii) the characteristics of sliding bubbles' trajectory after departing from a single nucleation site (section 4.2), and (iii) the temporal fraction of bubbles' residence throughout the heated wall (section 4.3).

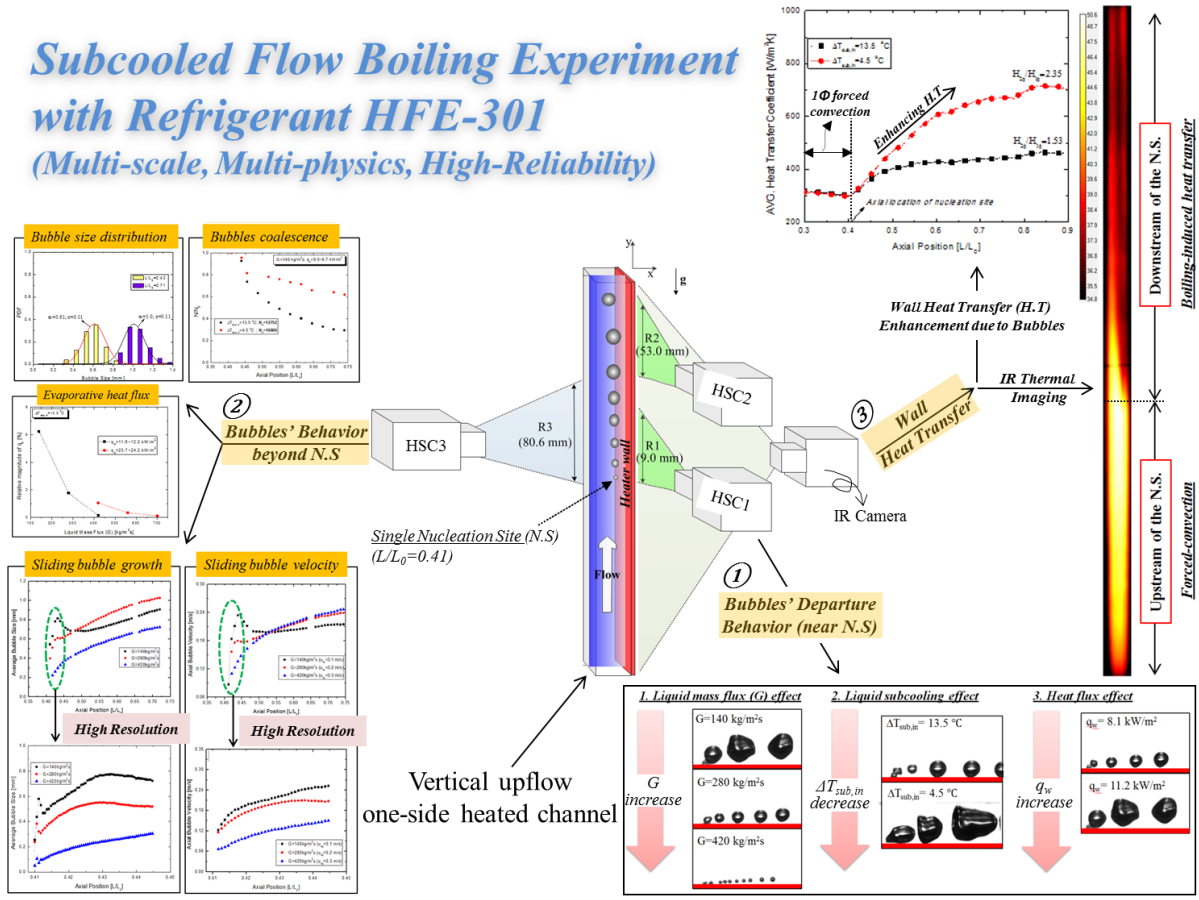

Figure 3. Measurement strategy and available research scope from the present subcooled flow boiling experiment

IV. RESULTS AND DISCUSSION

4.1. Growing Wall Heat Transfer due to Sliding Bubbles

The significance of sliding bubbles' effect on wall heat transfer is well presented in Figure 4. It shows that after a boiling occurrence at the single nucleation site located at $L/L_0 \approx 0.41$ the wall heat transfer coefficient (h) increased abruptly while there was a sharp drop in wall temperature (T_w). The T_w and the h shown are averaged values across the heater width at each axial location (*i.e.*, $q'' = h \cdot (T_w - T_{bulk})$). Considering no nucleation site exists downstream of $L/L_0 \approx 0.41$, it is obvious that the wall heat transfer was enhanced by the sliding vapor bubbles emanating from the single nucleation site.

In Tables 1 and 2, the degree of wall heat transfer enhancement induced by sliding bubbles relative to single-phase forced convection ($H_{2\Phi}/H_{1\Phi}$) is compared at different test conditions ($H_{2\Phi}$ is time-averaged wall heat transfer coefficient measured at $L/L_0 \approx 0.9$ under influence of sliding bubbles while $H_{1\Phi}$ was measured at $L/L_0 \approx 0.3$ upstream of the nucleation site, see Figure 4). Table 1 shows the values of $H_{2\Phi}/H_{1\Phi}$ depending on mass flux (G) through the test channel while the effects of inlet subcooling ($\Delta T_{sub,in}$) on $H_{2\Phi}/H_{1\Phi}$ are shown in Table 2. It is obvious from Tables 1 and 2 that the degree of wall

heat transfer enhancement, *i.e.*, $H_{2\Phi}/H_{1\Phi}$ decreased as G and $\Delta T_{sub,in}$ increased. Regarding this observation, we revealed in our previous study [7] that both the sliding bubble growth behavior near the nucleation site and the relative velocity of sliding bubbles against the local flowing liquid played a critical role in determining $H_{2\Phi}/H_{1\Phi}$.

However, while analyzing the bubbles' sliding characteristic in different aspect, we additionally found that the trajectories of sliding bubbles (or spatial distribution of sliding bubbles during the measurement period) should also be carefully investigated to understand the effect of sliding bubbles on wall heat transfer. For instance, if the sliding bubbles travel downstream through various paths (or trajectories), the influential area of sliding bubbles will become larger than that when the bubbles go through a single path; on the other hand, the sliding bubbles' impact on wall heat transfer per unit area within the sliding paths will become less because the effect spread over wider area instead of being concentrated. What was observed from the present experiment is that the smaller sliding bubbles at higher G or at higher $\Delta T_{sub,in}$ tended to spread more in lateral direction relative to their size. Therefore, to draw better conclusion on the relation between sliding bubble characteristics and associated wall heat transfer, we need to better understand the sliding bubbles' trajectory in subcooled boiling flow, the detailed and quantitative analyses of which are given in sections 4.2 and 4.3.

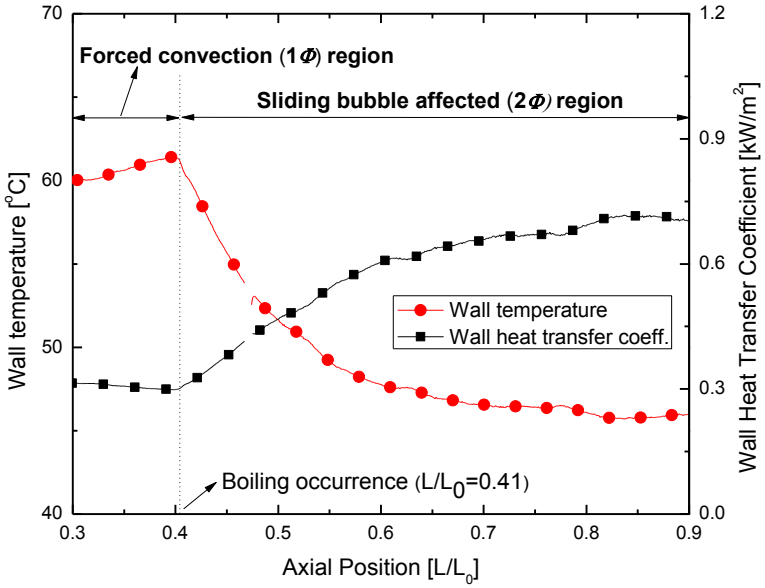

Figure 4. Wall temperature and wall heat transfer variations induced by sliding bubbles originating from a single nucleation site (q_w=9.5 kW/m^2, $\Delta T_{sub,in}$=4.5 °C, G=140 kg/m^2/s)

Table 1. Effects of mass flux (G) on $H_{2\Phi}/H_{1\Phi}$

q_w=11.6–12.2 kW/m^2, $\Delta T_{sub,in}$ (°C)=13.5 °C		q_w=23.7–24.2 kW/m^2, $\Delta T_{sub,in}$ (°C)=13.5 °C	
G (kg/m^{2}s)	**$H_{2\Phi}/H_{1\Phi}$**	G (kg/m^{2}s)	**$H_{2\Phi}/H_{1\Phi}$**
140	1.64	420	1.23
280	1.29	560	1.12
420	1.12	700	1.10

Table 2. Effects of inlet subcooling ($\Delta T_{sub,in}$) on $H_{2\Phi}/H_{1\Phi}$

G=140 kg/m^{2}s, q_w=9.5–9.7 kW/m^2		G=420 kg/m^{2}s, q_w=20.1–20.4 kW/m^2		G=700 kg/m^{2}s, q_w=30.5–30.9 kW/m^2	
$\Delta T_{sub,in}$ (°C)	**$H_{2\Phi}/H_{1\Phi}$**	$\Delta T_{sub,in}$ (°C)	**$H_{2\Phi}/H_{1\Phi}$**	$\Delta T_{sub,in}$ (°C)	**$H_{2\Phi}/H_{1\Phi}$**
13.5	1.53	13.5	1.18	13.5	1.11
4.50	2.35	4.50	1.40	4.50	1.15

Another interesting finding for the sliding bubbles' effect on wall heat transfer is that as shown in Figure 5 $H_{2\Phi}/H_{1\Phi}$ was affected less by the changes in Ja (or wall superheat degree) at higher mass flux (G) conditions. That is, $H_{2\Phi}/H_{1\Phi}$ varied less at higher G despite the significant changes in wall superheat condition (*i.e.*, Ja) while the degree of wall heat transfer enhancement $H_{2\Phi}/H_{1\Phi}$ became low as G increased (Table 1). It is worth noting here that these results are very similar with those obtained in air-bubble injection experiments (non-boiling) performed by Kenning and Kao [11] and Thorncroft and Klausner [3]. This similarity between vapor and gas sliding bubbles implies that in addition to the vapor bubble characteristics influenced by G (*e.g.*, sliding bubble growth due to evaporation), some other physics like liquid turbulence enhancement caused by sliding bubbles can also contribute substantially to the wall heat transfer improvement [12, 13] as well as determining the trend shown in Figure 5. In this paper, we argue that the sliding bubble trajectory is another physics to pay attention (sections 4.2 and 4.3).

Lastly, it is also interesting to note that in our previous study [7] the bubble release frequency from a single nucleation site was found to vary more sensibly by the changes in wall superheat condition (or Ja) at higher mass fluxes (G), which is opposite to that shown in Figure 5.

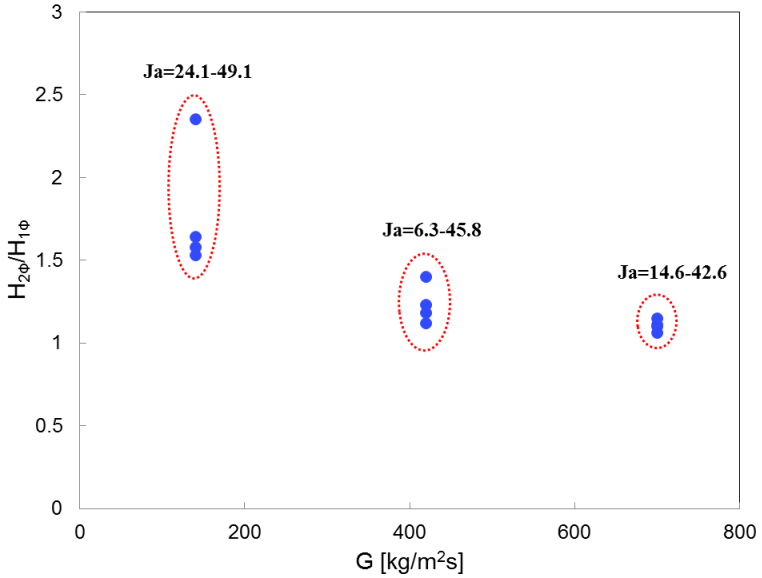

Figure 5. Variation of $H_{2\Phi}/H_{1\Phi}$ influenced by wall superheat condition (Ja) depending on mass flux (G)

4.2. Sliding Bubbles' Trajectory and Wall Area of Bubble Influence

This section discusses the sliding bubbles' effect on wall heat transfer based on the investigation of the sliding bubbles' trajectory at subcooled flow boiling conditions. Figure 6 shows the general approach taken in CFD modelling [4, 5] to address the sliding bubbles' effect on wall heat transfer, assuming a straight and single path of sliding bubbles from a nucleation site. However, the present observation revealed that the bubbles emanating from a single nucleation site slid through various paths and the wall area swept by the sliding bubbles was often substantially larger than that covered by a single path. This implies that the wall area influenced by sliding bubbles at a given subcooled flow boiling condition is not just a function of bubble size (*e.g.*, $A_b = KN\dfrac{\pi D_b^2}{4}$ in Kurul and Podowski's wall heat flux partitioning model [8]) but also closely related to the sliding bubbles' trajectory. Thus, to clarify the unknown physics concerning the influential area of sliding bubbles in subcooled boiling flow, the characteristic of sliding bubbles' trajectory along the heated wall must be understood better.

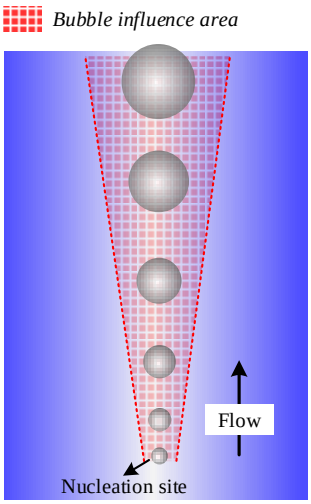

CFD models to address sliding bubble effect

Figure 6. Sliding bubble trajectory assumed in CFD models

In this regard, efforts were made to quantify the characteristic of sliding bubbles' trajectory, for which sliding bubbles' spreading factor S and bubble influence factor K are defined as follows:

$$S = \frac{Area\ swept\ by\ sliding\ bubbles}{D_{avg} \times l_s} \quad (1)$$

(where S is the sliding bubble spreading factor; D_{avg} is the average sliding bubble diameter within the sliding distance; l_s is the sliding distance)

$$K = \frac{A_i}{D_{avg} \times l_s} \quad (2)$$

(where K is the bubble influence factor; A_i is the wall area influenced by sliding bubbles)

The bubble spreading factor S represents how widely the sliding bubbles released from the single nucleation site spread in lateral direction relative to the bubble size while travelling. It is noted that the numerator in Eq. (1) '*area swept by sliding bubbles*' was obtained by analyzing the bubbles' trajectories captured from the top of sliding bubbles with the heater wall defined as the bottom (HSC 3, see Figure 3); D_{avg} in Eqs. (1) and (2) was obtained using the observation from both HSC 1 (near nucleation site) and HSC 3 (downstream) (see Figure 7 below). In particular, to characterize the *'area swept by sliding bubbles'* during the measurement period (80 sec) 40,000 images, specifically binary images achieved through image processing [6] were analyzed at each test condition. For the bubble influence factor K which determines the effective area thermally influenced by sliding bubbles, A_i in Eq. (2) was evaluated based on the thermal images (1,700 images were analyzed at each test) obtained from IR camera (see Figure 3). In Figure 7, the evaluation of S and K using both sliding bubble images and IR thermal images taken during the present work is illustrated.

The results obatained at 4 different test conditions, shown in Table 3, revealed both S and K were closely related to the sliding bubble size (D_{avg}). Specifically, S evaluated within the region $0.41 \le L/L_0 \le 0.43$ decreased as D_{avg} became larger, and the similar relation was found between K and D_{avg}. In addition, when comparing the present results for K with the values reported in literature for departing or lifting-off bubbles (*i.e.*, K=4 for Han, Griffith [14], K=1.8 for Judd and Hwang [15]) which have still been widely adopted [5, 8, 16-18], it was found that K values measured in this work were often observed larger especially for the smaller sliding bubbles. This is due to the fact that the wall area swept by smaller bubbles (sliding paths or trajectories) was larger compared to the sliding bubble size (D_{avg}) as S values in Table 3 imply (see Eq. (1)). Also, this result obviously pinpoints the deficiency of existing approach for the bubble influence factor K for the sliding bubbles in CFD

analyses of flow boiling system (Figure 6). It is noted that we are currently analyzing more data taken during this study in order to generalize the above-mentioned conclusion with more confidence.

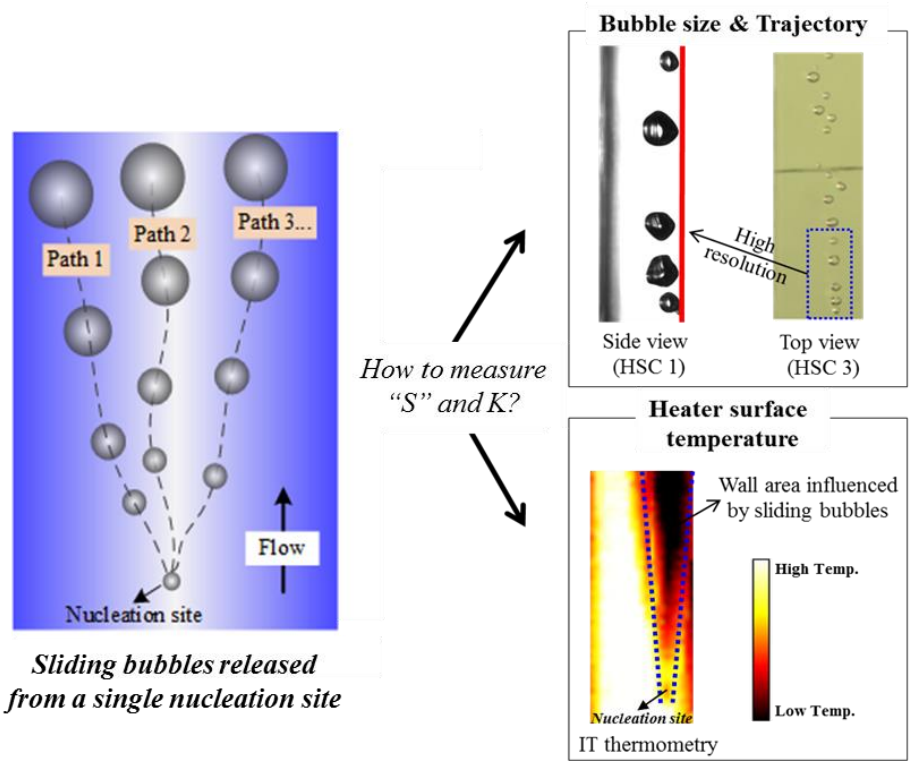

Figure 7. Measurement of sliding bubble spreading area (*S*) and bubble influence area (*K*)

Table 3. Sliding bubble size (D_{avg}), *S* and *K measured* at different subcooled flow boiling conditions within the sliding distance 4.5 mm from the nucleation site

Test condition	D_{avg} [mm]	*S*	*K*
G=140 kg/m^{2}s; q_w=9.5 kW/m^2; $T_{sub,in}$=4.5 ˚C	0.82	1.73	3.4
G=140 kg/m^{2}s; q_w=11.6 kW/m^2; $T_{sub,in}$=13.6 ˚C	0.62	2.14	4.3
G=420 kg/m^{2}s; q_w=23.7 kW/m^2; $T_{sub,in}$=13.5 ˚C	0.34	3.14	7.5
G=700 kg/m^{2}s; q_w=24.2 kW/m^2; $T_{sub,in}$=13.5 ˚C	0.17	6.4	13.8

4.3. Temporal Fraction of Bubble Residence

Another characteristic of bubbles' sliding behavior that has been investigated in conjunction with the sliding bubbles' trajectory is the temporal fraction of bubbles' residence throughout the heated wall during the measurement period (hereafter, F_R). This is important in the sense that F_R provides detailed information on both the area swept by sliding bubbles during measurement period and the 'effective' sliding bubble frequency passing through that area, which will directly affect the wall heat transfer mode like quenching or micro-convection influenced by sliding bubbles [5]. The two types of F_R can be defined as follows:

$$\overline{F_R}(y) = \int_0^{S_0} \overline{F_R}(y,z)dz \Big/ \int_0^{S_0} dz \tag{3}$$

(where $\overline{F_R}(y,z)$ is the temporal fraction of bubble residence during the measurement period at a location (y,z) on the heater wall; $\overline{F_R}(y)$ is the average temporal fraction of bubble residence at axial

location y; S_0 is the heater width swept by sliding bubbles at a given axial location)

$$\overline{F_R} = \int_0^{l_s}\int_0^{S_0} \overline{F_R}(y,z)dydz \Big/ \int_0^{l_s}\int_0^{S_0} dydz \quad (4)$$

(where $\overline{F_R}$ is the area-averaged time fraction of bubble residence within sliding distance l_s)

It is noted that the recording speed of high-speed camera (*i.e.*, HSC 3) should be low enough to take independent samples of sliding bubbles at a given location of the heater wall per each frame, which is essential to ensure the high statistical significance of F_R evaluated using Eqs. (3) and (4).

Figure 8 shows how the sliding bubble path and $\overline{F_R}(y,z)$ typically varied along the flow path after the bubbles departed from the single nucleation site (axial location of nucleation site: $L/L_0 \approx 0.41$). The bubbles slid through narrow path with high $\overline{F_R}(y,z)$ near the nucleation site, whereas the sliding bubbles swept wider area and $\overline{F_R}(y,z)$ decreased as the bubbles travelled downstream. This means that at the downstream region less number of sliding bubbles passed "per unit area" of bubble influence although the influential area of sliding bubbles became larger. Thus, the sliding bubbles' effect "per unit area" can be limited. This sliding bubbles' characteristic caused larger wall temperature gradient across the heater width near the nucleation site while such gradient significantly smeared out downstream [9]. That is, the sliding bubbles' impact on wall heat transfer was noticeable near the nucleation site but the influence was restricted to relatively narrow region; and this observation became reversed downstream. Also, we can expect from this observation that the wall heat transfer mode like quenching or micro-convection heat transfer induced by sliding bubbles [5] will depend on the distance from nucleation site.

Figure 9 shows the relation between $\overline{F_R}$ (see Eq. (4)) and bubble spreading factor S obtained through this work. We can see here that $\overline{F_R}$ decreased as S increased and the relation was consistent regardless of the sliding distance l_s. Considering that S has proportional relation with K (see Table 3), the similar relation is also expected between $\overline{F_R}$ and K. Another finding from Figure 9 is that S was estimated higher as the sliding distance (l_s^*) increased which is due to the fact that bubbles slid through wider path as they travelled downstream as discussed before.

In Figure 10, the increase in wall heat transfer through the bubbles' sliding distance $l_s^*=11.8$ depending on $\overline{F_R}$ is shown, the results of which were taken at 14 different test conditions. The result shown indicates that higher $\overline{F_R}$ tended to cause higher increase in wall heat transfer ($H_{downstream}/H_{upstream}$). From this, we can conclude that $\overline{F_R}$ significantly affected the degree of wall heat transfer enhancement induced by sliding bubbles, and $\overline{F_R}$ is strongly dependent on the characteristic of sliding bubbles' trajectory like S (see Figure 9). As discussed, $\overline{F_R}$ is physically related to the quenching or micro-convection heat transfer caused by sliding bubbles within the wall area of bubble influence.

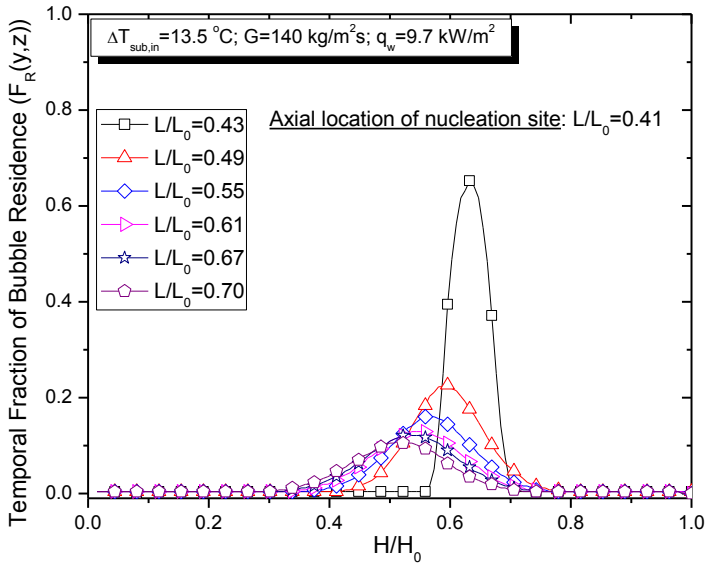

Figure 8. A typical development of $\overline{F_R}(y,z)$ along the flow path (H_0 is heater width (=7.5 mm) and H is horizontal position within H_0)

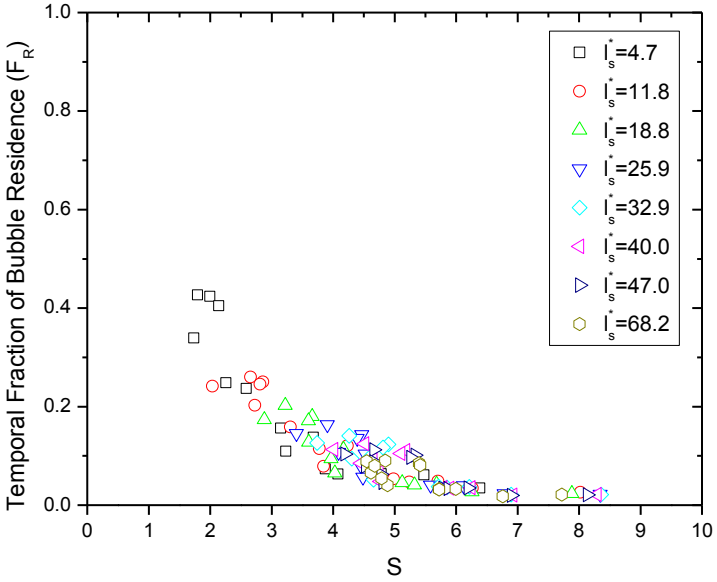

Figure 9. Observed relation between $\overline{F_R}$ and S ($l_s^* = l_s/\sqrt{\sigma/(g\Delta\rho)}$)

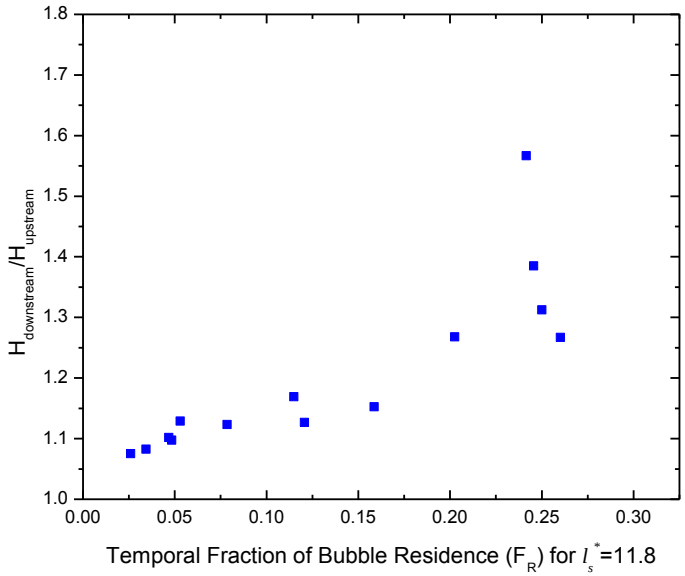

Figure 10. Degree of wall heat transfer enhancement ($H_{downstream}/H_{upstream}$) through the sliding distance l_s^*=11.8 depending on F_R

V. SUMMARY AND CONCLUSIONS

The effect of sliding bubbles on wall heat transfer in subcooled boiling flow is discussed in two different aspects: (i) wall heat transfer enhancement in relation to sliding bubble characteristics (supplementary discussion to authors' previous work) and (ii) wall area influenced by sliding bubbles.

The wall heat transfer at the region under influence of sliding bubbles was significantly enhanced relative to that under influence of single-phase forced convection, and the level of enhancement $H_{2\Phi}/H_{1\Phi}$ became higher as inlet subcooling degree or mass flux decreased. Regarding this observation, besides the sliding bubble characteristics discussed in our previous study [7], the sliding bubbles' trajectory is also claimed as an important factor to be addressed. Another finding concerning the wall heat transfer enhancement due to sliding bubbles is that $H_{2\Phi}/H_{1\Phi}$ varied less according to the changes in wall superheat condition (or Ja) at higher mass flux conditions.

The present analyses on sliding bubbles' trajectory revealed that the bubbles slid through various paths, and hence the wall area influenced by sliding bubbles was observed substantially larger than those reported in the previous studies. Also, the wall area influenced by sliding bubbles was not only a function of bubble size but also closely related to the sliding bubbles' trajectory. Meanwhile, both bubble spreading factor (S) and bubble influence factor (K) were found to be significantly influenced by the sliding bubble size. Specifically, the larger sliding bubbles showed less variation in their trajectories relative to the bubble size, resulting in smaller values of *S* and *K*. All the results clearly indicate the deficiency of existing approach for the area of bubble influence taken in the CFD analyses especially for flow boiling systems involving sliding bubbles.

Lastly, the sliding bubbles' characteristic was also discussed based on the analyses of temporal fraction of bubbles' residence (F_R) along the (heated) wall. The results show that bubbles typically slid through narrow path with high F_R near the nucleation site, whereas the sliding bubbles swept wider area and F_R became lower as the bubbles slid downstream. This caused a distinct decrease in wall temperature around the sliding bubbles' path near the nucleation site while the wall temperature gradient across the heater width significantly smeared out as the bubbles slid downstream. The results also imply that the quenching heat transfer mode caused by sliding bubbles is expected to show similar behavior depending on the distance from nucleation site.

It is hoped that the experimental findings discussed in this paper help improve our insight into the

bubbles' sliding characteristics and the thermal effect for advanced modelling.

ACKNOWLEDGMENTS

This research was supported by CASL (Consortium for Advanced Simulation of Light Water Reactors), an Energy Innovation Hub for Modeling and Simulation of Nuclear Reactors under U.S. Department of Energy Contract No DE-AC05-00OR22725. The support is gratefully acknowledged.

REFERENCES

1. Cornwell, K., *The influence of bubbly flow on boiling from a tube in a bundle.* International Journal of Heat and Mass Transfer, 1990. **33**(12): p. 2579-2584.
2. Houston, S. and K. Cornwell, *Heat transfer to sliding bubbles on a tube under evaporating and non-evaporating conditions.* International journal of heat and mass transfer, 1996. **39**(1): p. 211-214.
3. Thorncroft, G. and J. Klausner, *The influence of vapor bubble sliding on forced convection boiling heat transfer.* Journal of Heat Transfer, 1999. **121**(1): p. 73-79.
4. Basu, N., G.R. Warrier, and V.K. Dhir, *Wall heat flux partitioning during subcooled flow boiling: Part 1—Model development.* Journal of heat Transfer, 2005. **127**(2): p. 131-140.
5. Yeoh, G., et al., *Fundamental consideration of wall heat partition of vertical subcooled boiling flows.* International Journal of Heat and Mass Transfer, 2008. **51**(15): p. 3840-3853.
6. Yoo, J., C.E. Estrada-Perez, and Y.A. Hassan, *Experimental Study on Bubble Dynamics and Wall Heat Transfer Arising from a Single Nucleation Site at Subcooled Flow Boiling Conditions – Part 1: Experimental Methods and Data Quality Verification.* International Journal of Multiphase Flow, 2016. doi: 10.1016/j.ijmultiphaseflow.2016.04.018
7. Yoo, J., C.E. Estrada-Perez, and Y.A. Hassan, *Experimental Study on Bubble Dynamics and Wall Heat Transfer Arising from a Single Nucleation Site at Subcooled Flow Boiling Conditions – Part 2: Data Analysis on Sliding Bubble Characteristics and Associated Wall Heat Transfer.* International Journal of Multiphase Flow, 2016. doi:10.1016/j.ijmultiphaseflow.2016.04.019.
8. Kurul, N. and M.Z. Podowski. *Multidimensional effects in forced convection subcooled boiling*. in *Proceedings of the 9th International Heat Transfer Conference*. 1990. Jerusalem, Israel: Hemisphere Publishing Corporation.
9. Yoo, J., C.E. Estrada-Perez, and Y.A. Hassan, *An accurate wall temperature measurement using infrared thermometry with enhanced two-phase flow visualization in a convective boiling system.* International Journal of Thermal Sciences, 2015. **90**: p. 248-266.
10. Yoo, J., C.E. Estrada-Perez, and Y.A. Hassan, *A proper observation and characterization of wall nucleation phenomena in a forced convective boiling system.* International Journal of Heat and Mass Transfer, 2014. **76**: p. 568-584.
11. Kenning, D. and Y. Kao, *Convective heat transfer to water containing bubbles: enhancement not dependent on thermocapillarity.* International Journal of Heat and Mass Transfer, 1972. **15**(9): p. 1709-1717.
12. Yan, Y. and D. Kenning, *Flow boiling in bubbly flow*. 1996: Taylor and Francis, Washington, DC.
13. Yan, Y., D. Kenning, and K. Cornwell, *Sliding and sticking vapour bubbles under inclined plane and curved surfaces.* International Journal of Refrigeration, 1997. **20**(8): p. 583-591.
14. Han, C.-Y., P. Griffith, and C. Yeh. *The mechanism of heat transfer in nucleate pool boiling II*. in *International Journal of Heat and Mass Transfer*. 1965. Citeseer.
15. Judd, R. and K. Hwang, *A comprehensive model for nucleate pool boiling heat transfer including microlayer evaporation.* Journal of Heat Transfer, 1976. **98**(4): p. 623-629.
16. Krepper, E. and R. Rzehak, *CFD for subcooled flow boiling: Simulation of DEBORA experiments.* Nuclear Engineering and Design, 2011. **241**(9): p. 3851-3866.
17. Bae, B.-U., et al., *Analysis of subcooled boiling flow with one-group interfacial area transport equation and bubble lift-off model.* Nuclear Engineering and Design, 2010. **240**(9): p. 2281-

2294.
18. Tu, J. and G. Yeoh, *On numerical modelling of low-pressure subcooled boiling flows.* International Journal of Heat and Mass Transfer, 2002. **45**(6): p. 1197-1209.